Theoretical Study on the Mechanism of the Dissociation of Benzene. The $C_5H_3 + CH_3$ Product Channel

A. M. Mebel,* S. H. Lin, X. M. Yang, and Y. T. Lee

Institute of Atomic and Molecular Sciences, Academia Sinica, P.O. Box 23-166, Taipei 10764, Taiwan, Republic of China

Received: February 17, 1997; In Final Form: March 28, 1997⊗

Potential energy surfaces for the various mechanisms of the dissociation of C_6H_6 producing different isomers of the C_5H_3 radical have been investigated using the *ab initio* modified Gaussian-2 (G2M) method. The most stable structures of C_5H_3, $H_2CCCCCH$ (**II1**) and HCCC(H)CCH (**II2**), can be formed from benzene and fulvene through the pathways involving a 1,2-H shift in the carbon ring and the ring opening followed by the series of hydrogen shifts in the open chain structures of C_6H_6. The reaction is completed by the elimination of CH_3 from $C_5H_3-CH_3$. All the transition states along the reaction pathways are found to lie below ~143 kcal/mol relative to benzene, while the heats of the reactions, benzene → $H_2CCCCCH + CH_3$ and benzene → HCCC(H)CCH + CH_3, are calculated to be about 150 kcal/mol. On this basis, the $C_5H_3 + CH_3$ product channel of the photofragmentation of benzene at 248 nm is expected to be a two-photon process. In total, 25 different isomers of C_5H_3 have been calculated. The most stable, **II1** and **II2**, are predicted to have the enthalpies of formation of 136.5 and 137.2 kcal/mol, respectively. Contrary to $C_5H_3^+$, the ethynyl cyclopropenyl isomer of neutral C_5H_3 is only the third in stability with a $\Delta H_f(298)$ of 166.9 kcal/mol.

Introduction

Molecular beam studies of the photodissociation of benzene at 193 and 248 nm have shown that one of the primary fragmentation channels at both wavelengths is $C_5H_3 + CH_3$.[1] Neutral CH_3 fragments have also been observed in the electron impact ionization of benzene.[2] In order to produce C_5H_3 and CH_3, H atoms in benzene must migrate until one carbon gathers three H atoms and the CC bond breaks. Considering the energetics of C−C bond rupture (80−90 kcal/mol), excitation at 248 nm, which deposits 115 kcal/mol in the molecule, seems to be insufficient to break apart the benzene ring. However, H migration and isomerization could take place at this energy and only formation of an isomer containing a single C−C bond, $C_5H_3-CH_3$, will lead to C−C bond rupture. Accumulation of three H atoms on a terminal carbon is the key to C−C bond rupture and CH_3 formation. The mechanism of the rearrangement of benzene to a $C_5H_3-CH_3$ isomer and the structure and energetics of the C_5H_3 radical formed after the C−C bond cleavage require clarification.

The $C_5H_3^+$ cation is commonly observed in mass spectra.[3−12] For instance, it is formed during electron impact[4,8,12] and laser multiphoton ionization/dissociation[6,10] of hexadienes and benzyl derivatives, during photoion fragmentation of naphthalene and azulene monocations,[9] in the reaction of C^+ with benzene,[13] etc. The cation is also believed to be an important intermediate of soot formation in the fuel-rich flames.[14] The structure and stability of various isomers of $C_5H_3^+$ have been well studied theoretically using semiempirical[8,12] and *ab initio* molecular orbital (MO) calculations.[10,15,16] The information about the neutral C_5H_3 radical is scarce. Kuehnel and co-workers[17] carried out semiempirical MINDO/3 calculations for various structures of C_5H_3. Pasto considered some open-chain structures of the radical at the HF and MP2 levels.[18] Melius calculated the heats of formation for several C_5H_3 isomers using the BAC-MP4 method.[19]

From the experimental data,[1] it is difficult to unambiguously conclude whether the formation of C_5H_3 from benzene is the result of one-photon or two-photon excitation. High-level *ab initio* MO calculations can provide accurate energetics for the $C_6H_6 \rightarrow C_5H_3 + CH_3$ reaction. Comparison of the calculated reaction endothermicity with the photon energy will assist in solving the problem. As discussed in the following section, the computational method used, modified Gaussian-2 (G2M),[20] usually provides an accuracy within a few kcal/mol for the relative energies of the local minima and transition states along potential energy surfaces (PES) of the reactions of medium size molecules and radicals of the first row. Recently,[21] we have employed the G2M method for the calculations of PES for the benzene → fulvene isomerization reaction.

Besides the requirement that the calculated energies should be accurate, it is necessary to find the global minimum on PES of the C_5H_3 species, i.e., to locate the lowest in energy isomer. In order to reach this goal, we systematically study nearly all possible geometric configurations of C_5H_3 which are divided into several groups according to the arrangement of the carbon atoms. Next, we consider PES for various reaction mechanisms leading from benzene to the $C_5H_3 + CH_3$ products.

Computational Methods

The geometries of various isomers of the benzene molecule and C_5H_3 radical as well as transition states for the $C_6H_6 \rightarrow C_5H_3 + CH_3$ reaction have been optimized using the hybrid density functional B3LYP method, i.e., Becke's three-parameter nonlocal-exchange functional[22] with the nonlocal correlation functional of Lee, Yang, and Parr,[23] with the 6-311G(d,p) basis set.[24] Vibrational frequencies, calculated at the B3LYP/6-311G(d,p) level, have been used for characterization of stationary points and zero-point energy (ZPE) correction without scaling. All the stationary points have been positively identified for minimum (number of imaginary frequencies NIMAG = 0) or transition state (NIMAG = 1). All the energies quoted and discussed in the present paper include the ZPE correction.

⊗ Abstract published in *Advance ACS Abstracts,* July 1, 1997.

S1089-5639(97)00596-3 CCC: $14.00

TABLE 1: Relative Energies (kcal/mol) of Various Isomers of C_5H_3, C_6H_6, and Transitions States along the $C_6H_6 \rightarrow C_5H_3 + CH_3$ Reaction, Calculated at Different Levels of Theory

		B3LYP/ 6-311G(d,p)		RCCSD(T)/ 6-31G(d,p)		G2M(rcc,MP2)					B3LYP/ 6-311G(d,p)		RCCSD(T)/ 6-31G(d,p)		G2M(rcc,MP2)		
species	ZPE[a]	E_{rel}[b]	$E_{\mathrm{rel}}(B)$[c]	E_{rel}[b]	$E_{\mathrm{rel}}(B)$[c]	E_{rel}[b]	$E_{\mathrm{rel}}(B)$[c]	ΔH_f[d]	species	ZPE[a]	E_{rel}[b]	$E_{\mathrm{rel}}(B)$[c]	E_{rel}[b]	$E_{\mathrm{rel}}(B)$[c]	E_{rel}[b]	$E_{\mathrm{rel}}(B)$[c]	ΔH_f[d]
C_5H_3																	
I1	33.7	53.7	189.5	39.1	188.5	42.9	193.4	178.2	**III1**	31.6	35.3	171.2	31.7	181.1	30.3	180.9	166.9
I2	33.5	48.7	184.6	33.5	182.9	32.9	183.5	168.5	**III2**	33.1	49.2	185.1					
I3	32.7	65.1	201.0	49.3	198.6	54.4	205.0	190.2	**III3**	33.4	50.5	186.4					
I4	33.6	73.8	209.6						**III4**	31.4	65.4	201.2	61.3	210.7	61.5	212.0	197.8
I5	33.8	83.6	219.4						**IV1**	33.8	49.4	185.3					
I6	33.8	78.4	214.2						**IV2**	32.5	70.5	206.4					
II1[e]	32.1	0.0	135.9	0.0	149.4	0.0	150.6	136.5	**IV3**	32.5	88.7	224.6					
II2	32.4	5.6	141.5	2.2	151.6	1.0	151.5	137.2	**IV4**	32.4	89.7	225.6					
II3	32.3	41.0	176.9						**IV5**	31.6	90.4	226.3					
II4	31.2	52.1	187.9						**IV6**	31.6	90.1	226.0					
II5	32.9	55.9	191.7	44.7	194.1	52.5	203.0	188.6	**V1**	33.9	83.2	219.1					
II6	32.5	63.5	199.4						**V2**	34.4	102.8	238.7					
II7	32.6	69.9	205.8														
C_6H_6																	
B1[f]	62.9		0.0		0.0		0.0	19.8	**B9**	59.1		81.0					
B2	61.2		33.8		31.5		30.2	48.8	**B9′**	58.9		82.8		85.6		83.8	104.8
B3	59.2		102.8		100.6		99.2	119.9	**B10**	58.4		70.1		79.4		76.6	98.1
B3o	58.7		96.1		95.9		100.6	121.4	**B11**	59.4		60.5		63.0		60.5	81.6
B4	58.3		120.4		118.8		122.9	143.7	**B11′**	59.6		64.8					
B5	59.6		94.5		95.2		92.4	112.8	**B12**	58.7		73.3		77.1		75.0	96.4
B6	59.2		101.6		99.4		97.9	118.5	**B13**	56.8		125.7		131.7		127.9	149.4
B7	58.2		71.3		77.6		75.0	96.3	**B13′**	56.9		122.7					
B7′	58.3		68.8						**B14**	60.3		90.1		91.1		88.8	
B8	58.9		63.5		70.3		68.0	89.2									
TS **1**	57.0		128.8		131.1		129.3		TS **10**	54.8		137.8		149.1		143.2	
TS **2**	57.0		146.1		146.2		141.4		TS **11**	55.3		158.0					
TS **3**	59.6		128.8						TS **12**	56.1		114.9		118.8		114.3	
TS **4**	57.9		105.7		106.4		101.7		TS **13**	55.2		140.1		146.8		140.9	
TS **5**	55.6		154.9						TS **14**	55.5		133.0		140.4		133.5	
TS **6**	58.0		112.9		115.4		111.3		TS **15**	54.4		144.0					
TS **7**	54.7		134.4		143.7		138.8		TS **16**	59.3		92.7		93.0		89.4	
TS **8**	55.0		131.0		142.4		136.0		TS **17**	57.9		110.5		112.6		110.7	
TS **9**	55.8		148.5		151.6		146.9										
$2C_3H_3$	51.4		135.3		148.7												

[a] Zero-point energy corrections (kcal/mol), calculated at the B3LYP/6-311G(d,p) level. [b] The energy relative to the most stable isomer of C_5H_3, **II1**. ZPE are included. [c] The energy relative to benzene; for C_5H_3, the energy of $C_5H_3 + CH_3$ relative to benzene. ZPE are included. [d] Heats of formation at 298 K, computed on the basis of the experimental $\Delta H_f(298)$ for benzene (19.8 kcal/mol, ref 31) and CH_3 (34.8 kcal/mol, ref 32) and calculated G2M relative energies and the B3LYP/6-311G(d,p) thermal correction to enthalpy. [e] The total energies in hartrees are as follows: B3LYP/6-311G(d,p), −192.218 91; RCCSD(T)/6-31G(d,p), −191.607 12; G2M(rcc,MP2), −191.791 51. [f] The total energies in hartrees are as follows: B3LYP/6-311G(d,p), −232.308 55; RCCSD(T)/6-31G(d,p), −231.580 51; G2M(rcc,MP2), −231.774 71.

In order to obtain more reliable energies of the most important equilibrium structures and transition states, we used the G2M(rcc,MP2)[20] method. The G2M(rcc,MP2) method is a modification of the Gaussian-2 (G2) approach[25] by Pople and co-workers; it uses B3LYP/6-311G(d,p) optimized geometries and ZPE corrections and substitutes the QCISD(T)/6-311G(d,p) calculation of the original G2 scheme by the restricted open-shell coupled cluster[26] RCCSD(T)/6-31G(d,p) calculation. The total energy in G2M(rcc,MP2) is calculated as follows:[20]

$$E[\mathrm{G2M(rcc,MP2)}] = E[\mathrm{PMP4/6\text{-}311G(d,p)}] + \Delta E(\mathrm{rcc}) + \Delta E(+\mathrm{3df2p}) + \Delta E(\mathrm{HLC}) + \mathrm{ZPE[B3LYP/6\text{-}311G(d,p)]}$$

where

$$\Delta E(\mathrm{rcc}) = \mathrm{E[RCCSD(T)/6\text{-}31G(d,p)]} - E[\mathrm{PMP4/6\text{-}31G(d,p)}]$$

$$\Delta E(+\mathrm{3df2p}) = E[\mathrm{MP2/6\text{-}311{+}G(3df,2p)}] - E[\mathrm{MP2/6\text{-}311G(d,p)}]$$

and the empirical "higher level correction"

$$\Delta E(\mathrm{HLC}) = -4.93 n_\beta - 0.19 n_\alpha$$

where n_α and n_β are the numbers of α and β valence electrons, respectively. It has been shown[20] that the G2M(rcc,MP2) method gives the average absolute deviation of 1.28 kcal/mol of calculated atomization energies from experiment for 32 first-row G2 test compounds. The GAUSSIAN 94[27] and MOLPRO 96[28] programs were employed for the calculations.

Results and Discussion

Isomers of the C_5H_3 Radical. Numerous topologically different structures of the C_5H_3 species may exist. They can be divided into several groups according to the arrangement of the carbon atoms: (i) five-member ring isomers; (ii) open chain isomers; (iii) three-member ring isomers; (iv) four-member ring isomers; (v) cage isomers with three-dimensional carbon skeleton; (vi) branching chain isomers. Within each group, the structures differ by the distribution of three hydrogen atoms. For example, in the five-member ring group, three H atoms can be located on three neighboring carbons, or two H's on two neighboring carbons and one H in the para-position to them, or two H atoms on the same carbon and the third one in either the ortho- or para-position. We consider here most of the topologically possible structures. We excluded the structures which have more than one two-valence (carbene-like) carbon atoms, assuming that such structures are high in energy. Twenty-five

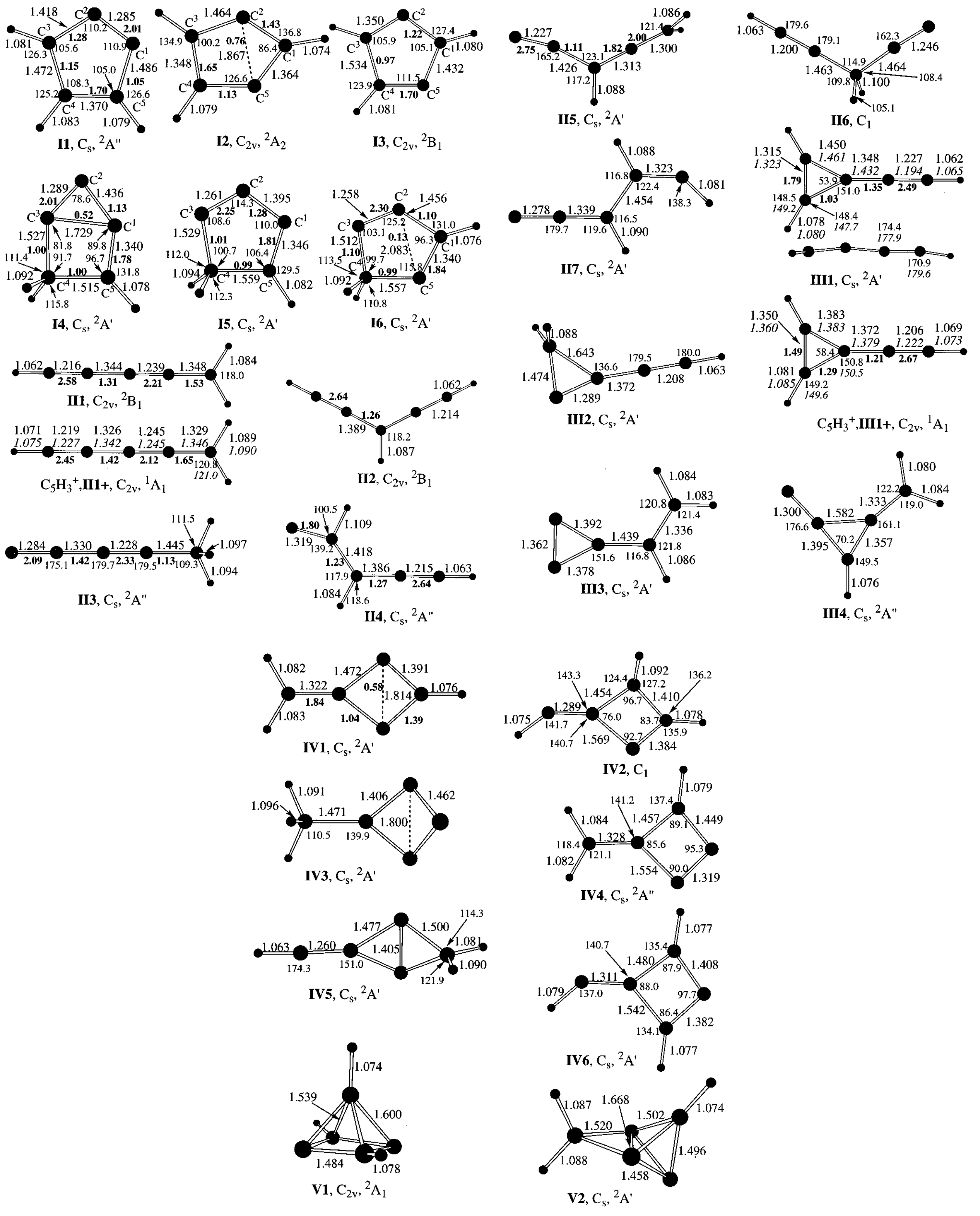

I1, C_s, $^2A''$ **I2**, C_{2v}, $^2A_2$ **I3**, C_{2v}, $^2B_1$ **II5**, C_s, $^2A'$ **II6**, C_1

I4, C_s, $^2A'$ **I5**, C_s, $^2A'$ **I6**, C_s, $^2A'$ **II7**, C_s, $^2A'$ **III1**, C_s, $^2A'$

II1, C_{2v}, $^2B_1$ $C_5H_3^+$,**II1+**, C_{2v}, $^1A_1$ **II2**, C_{2v}, $^2B_1$ **III2**, C_s, $^2A'$ $C_5H_3^+$,**III1+**, C_{2v}, $^1A_1$

II3, C_s, $^2A''$ **II4**, C_s, $^2A''$ **III3**, C_s, $^2A'$ **III4**, C_s, $^2A''$

IV1, C_s, $^2A'$ **IV2**, C_1 **IV3**, C_s, $^2A'$ **IV4**, C_s, $^2A''$ **IV5**, C_s, $^2A'$ **IV6**, C_s, $^2A'$

V1, C_{2v}, $^2A_1$ **V2**, C_s, $^2A'$

Figure 1. Geometries of various isomers of C_5H_3 and $C_5H_3^+$ optimized at the B3LYP/6-311G(d,p) level. (Bond lengths are in angstroms, bonds angles are in degrees.) For the structures **III1**, **II1+**, and **III1+** italic numbers show the MP2/6-31G(d) optimized geometric parameters. Bold numbers show Wiberg bond indices of C−C bonds in selected structures, calculated at the B3LYP/6-311G(d,p) level.

different isomers of C_5H_3 were found and their optimized geometries are shown in Figure 1. All the structures are local minima; they have no imaginary frequencies. The isomers belong to groups i−v, and no branching chain equilibrium structures were calculated. The energies of various isomers are presented in Table 1.

The most stable structure is **II1** (C_{2v},$^2B_1$), which can be described by the following resonance structures

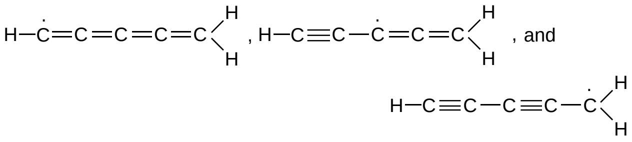

$$\mathrm{H{-}\dot{C}{=}C{=}C{=}C{=}CH_2},\quad \mathrm{H{-}C{\equiv}C{-}\dot{C}{=}C{=}CH_2},\ \text{and}\quad \mathrm{H{-}C{\equiv}C{-}C{\equiv}C{-}\dot{C}H_2}$$

The first of the three is a cumulene-like structure, the third one is a diyne, and the second one is a cumulene-acetylenic form.

According to the calculated geometry and Wiberg bond indices (WBI), shown in boldface in Figure 1, the electronic structure of **II1** is a mixture of the resonance structures. Another open chain isomer **II2** (C_{2v},$^2B_1$) or

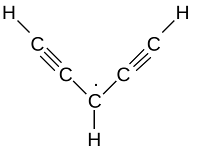

a typical diyne, lies only 1.0 kcal/mol higher than **II1** at the G2M(rcc,MP2) level. The relative stability of **II1** and **II2** is similar to that calculated for the corresponding isomers of the $C_5H_3^+$ cation.[10,16] However, in the cation these open chain structures are the second and the third isomers in the order of energies, about 20 kcal/mol higher than the most stable configuration of $C_5H_3^+$, ethynyl cyclopropenylium **III1+**. For the neutral radical, the ethynyl cyclopropenyl isomer **III1** lies 30.3 kcal/mol higher in energy than **II1** at the G2M level.

In order to confirm this conclusion, we additionally performed B3LYP/6-311G(d,p) geometry optimization for **II1+** and **III1+** and calculated their CCSD(T)/6-31G(d,p) energies. As seen in Figure 1, optimized geometries of **II1+** and **III1+** are almost identical at the B3LYP/6-311G(d,p) and MP2/6-31G(d) levels. In the RCCSD(T)/6-31G(d,p)//B3LYP/6-311G(d,p) approximation with ZPE corrections, **II1+** is higher than **III1+** by 15.1 kcal/mol, while **II1** is lower than **III1** by 31.7 kcal/mol. Thus, the presence or absence of one electron changes the relative stabilities of these structures by as much as 47 kcal/mol. Similarly, a comparison between the experimental heats of formation for the analogous cyclic cyclopropenyl cation and the linear propynyl cation shows that the cyclic cation is more stable by 25.1 kcal/mol, while the opposite case is true for the neutral species.[29]

Hehre *et al.*[30] suggested that the cyclopropenyl cation, $C_3H_3^+$, should exhibit considerable aromatic stabilization owing to delocalization of the two π electrons into the vacant p orbital at the carbocation center. One can use a similar argument for the ethynyl cyclopropenyl cation. The electronic structure of **III1+** is described by the following resonance structure

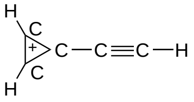

and all CC bond lengths in the ring and the adjacent CC bond length are almost equal. These CC bonds have WBI of 1.21−1.49, while the WBI of the acetylenic bond is 2.67. Thus, **III1+** is aromatically stabilized. In the neutral species **III1**, one electron is added into an antibonding orbital, which leads to the loss of aromaticity and a CC bond alteration. The structure slightly deviates from C_{2v} symmetry; only C_s symmetry with the mirror plane perpendicular to the plane of the cycle is maintained. The electronic structure can be described in terms of the acetylenic

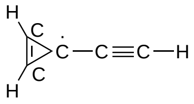

and cumulenic

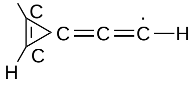

resonance structures, which is supported by the calculated WBI, shown in Figure 1. MP2/6-31G(d) and B3LYP/6-311G(d,p) optimized geometries for **III1** are close, but the MP2 method favors the acetylenic structure vs the cumulenic one. The B3LYP geometry is slightly preferable because the RCCSD(T)/6-31G-(d,p)//B3LYP energy of **III1** is 0.4 kcal/mol lower than the RCCSD(T)/6-31G(d,p)//MP2 energy.

For the linear species **II1** and **II1+** the electronic structures are similar, with a slightly higher contribution of the cumulenic resonance structures in the cation, as one can judge from the Wiberg bond indices.

Using the G2M calculated enthalpy of the C_6H_6 (benzene) → $C_5H_3 + CH_3$ reaction and the experimental heats of formation of benzene (19.8 kcal/mol)[31] and CH_3 (34.8 kcal/mol),[32] we compute $\Delta H_f(298)$ for C_5H_3 **II1**, **II2**, and **III1** as 136.5, 137.2, and 166.9 kcal/mol. For the linear structures **II1** and **II2**, BAC-MP4 enthalpies of formation, reported by Melius,[19] are 128.2 and 135.0 kcal/mol. The ionization potentials for **II1** and **III1**, calculated at the RCCSD(T)/6-31G(d,p) + ZPE level, are 175.0 and 128.1 kcal/mol, respectively. Therefore, the enthalpies of formation for the cationic **II1+** and **III1+** are estimated as 311.5 and 295.0 kcal/mol. $\Delta H_f(298)$ obtained for $C_5H_3^+$ **II1+** is in good agreement with the experimental value of 314−315 kcal/mol.[5,10]

The other open-chain isomers considered, **II3−II7**, are significantly less stable than **II1** and **II2** and lie 40−70 kcal/mol higher than **II1** at the B3LYP + ZPE level. The G2M calculated relative energy of **II5**, 52.5 kcal/mol, is close to the B3LYP value. Isomer **II3** can have the resonance

$$:C{=}C{=}C{=}\dot{C}{-}CH_3,\ :C{=}\dot{C}{-}C{\equiv}C{-}CH_3,\ \text{and}\ \dot{C}{\equiv}C{-}C{\equiv}C{-}CH_3$$

configurations. Due to the Jahn−Teller distortion, **II3** deviates from C_{3v} symmetry and its geometry is C_s symmetric. Isomer **II4** can be described by the

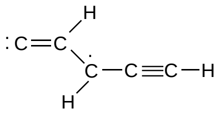

and

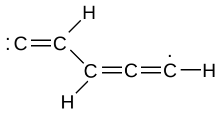

resonance structures, and according to WBI, the acetylenic structure dominates. Other than **III1** isomers from group iii, **III2−III4**, lie 49−65 kcal/mol higher than the global minimum **II1** at the B3LYP + ZPE level.

We found six different isomers belonging to group i and containing a five-member cycle, **I1−I6**. The most stable structure in this group is **I2** (C_{2v},$^2A_2$) which is 32.9 kcal/mol higher in energy than **II1**. The unpaired electron in **I2** is distributed between C^1, C^2, and C^5, and the corresponding resonance structures are

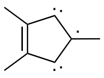

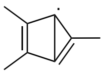

and

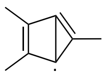

The C^2-C^5 distance across the ring is 1.87 Å, and the Wiberg bond index is 0.76, suggesting substantial bonding between these two atoms. Isomer **I3** is topologically similar to **I2**, but it does not have any across-ring C^2-C^5 bond. The electronic structure of **I3** can be described in terms of $C^2{=}C^3$ and $C^4{=}C^5$ double bonds and C^1-C^2, C^1-C^5, and C^3-C^4 single bonds, and the unpaired electron is localized on C^1. **I3** is 21.5 and 54.4 kcal/mol less stable than **I2** and **II1**, respectively, at the G2M level. Isomer **I1** is similar to *o*-benzyne. Three hydrogen atoms are connected to three neighboring carbons, and the electronic structure is described by the following resonance structures

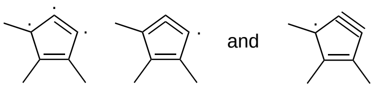

The quartet-like structure with three unpaired electrons (two of them have antiparallel spins) has the major contribution in the wave function, as seen from the WBI values. This is also supported by the high spin contamination of the wave function; the S^2 value at the B3LYP/6-311G(d,p) level before annihilation is 1.35 vs 0.75 for a pure doublet. **I1** lies 42.9 kcal/mol higher than the global minimum **II1**.

Three five-member ring isomers **I4**−**I6** having two H atoms at the same carbon (C^4) are substantially less stable than **II1** and even **I1**−**I3**; therefore, we carried out calculations for them only at the B3LYP level. In this approximation, they lie 74−84 kcal/mol higher than **II1**. The resonance structures describing **I4**−**I6** are the following

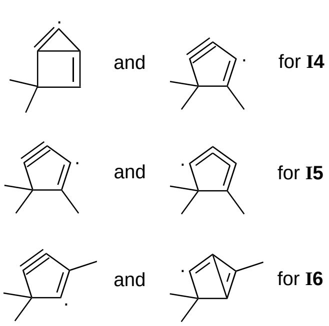

The Wiberg bond index for C^1-C^3 in **I4** is 0.52 suggesting a substantial across-ring bonding. On the other hand, in **I6** the Wiberg index for C^2-C^5 is only 0.13 and the across-ring bonding is weak.

In group iv, the most stable structure is **IV1**, 49.4 kcal/mol higher than **II1**, and other five isomers lie in the 70−90 kcal/mol energy range. The structures with three-dimensional carbon cages, pyramidal **V1** and bipyramidal **V2**, are very high in energy.

Summarizing, one can say that the relative stability of the neutral C_5H_3 isomers differs from that for the cation. The ethynyl cyclopropenyl structure is destabilized in the radical, and **III1** is only the third isomer of C_5H_3 in the energetic order. Close in energy open-chain structures **II1** and **II2** become the most stable isomers. The five-member ring configuration **I2** is 33 kcal/mol less stable than **II1**, while the cationic analog of **I2** was calculated to be 36 kcal/mol higher in energy than **II1+**.[10] The other cyclic structures **I4** and **I6** are destabilized in the neutral species; the relative energies of their cationic analogs with respect to **II1+** are 5−22 kcal/mol lower than the relative energies of **I4** and **I6** with respect to **II1**. For the open-chain structures, the relative stability of **II4** seems to be unchanged, while **II5** is stabilized by about 30 kcal/mol in the neutral species. However, only a qualitative comparison is warranted here because the levels of calculations used for C_5H_3 and $C_5H_3^+$ are different.

Mechanisms of the $C_6H_6 \rightarrow C_5H_3 + CH_3$ Reaction. The calculated endothermicity of the C_6H_6 (benzene) → C_5H_3 **II1** + CH_3 reaction is 150.6 kcal/mol at our best G2M level. At the B3LYP level, the heat of the reaction is 135.9 kcal/mol and BAC-MP4 calculations of Melius give the value of 142.3 kcal/mol.[19] At all levels of theory this energy is much higher than the energy available from the 248 nm photoexcitation. We consider below various mechanisms of formation of the different $C_5H_3-CH_3$ isomers from benzene (**B1**). First, we studied the pathways leading to $C_5H_3-CH_3$ from fulvene (**B2**) which seems to be a suitable precursor because two H atoms in fulvene are already collected on one out-of-ring carbon and only migration of one additional hydrogen is needed to form a $C_5H_3-CH_3$ isomer. It is well-known from experiment[33] and theoretical considerations[34,35] that the photoexcitation of benzene molecule to S_1 ($^1B_{2u}$) or S_2 ($^1B_{1u}$) states can lead to its isomerization to fulvene. The mechanism of this photochemical valence isomerization has also been explored. Recently, we calculated the ground state potential energy surface for various mechanisms of the benzene → fulvene rearrangement at the G2M level and found that the highest barrier on the isomerization pathway is ∼105 kcal/mol relative to benzene.[21] Optimized geometries of the C_6H_6 isomers and transition states are shown in Figures 2 and 3, respectively. Reaction mechanisms leading to different configurations of the C_5H_3 radical are presented in Figures 4a−d. The energies of various species along the reaction pathways are collected in Table 1. We also show in the figures the G2M and B3LYP + ZPE (italics) relative energies with respect to benzene.

The cyclic isomer **I1** can be formed by the following mechanism: fulvene **B2** → TS **1** → **B3** → **I1** + CH_3, which involves the 1,3-hydrogen shift in fulvene followed by the cleavage of the out-of-ring CC bond. The barrier for the hydrogen shift at TS **1** is 99.1 kcal/mol at the G2M level, and **B3** lies 69.0 kcal/mol higher than **B2**. The CC bond strength in **B3** is 94 kcal/mol, and the overall endothermicity of the **B1** → **I1** + CH_3 reaction is 193.4 kcal/mol, much higher than the energy of a 248 nm photon. The elimination of CH_3 takes place without barrier; the reverse reaction is a barrierless association of two radicals. We calculated isomer **B3** in two electronic states. One is the ^1A closed shell structure without symmetry, and the second is the open shell singlet $^1A''$ structure **B3o** which possesses C_s symmetry. Geometries of the C_5 ring in **B3** and **B3o** differ by the positions of the double bonds. One of the CCC angles in the ring of **B3** is 94.7°, which suggests across-ring electron sharing, and the trans-annular length is 2.05 Å. In **B3o**, one unpaired electron is located on the π orbital of the C atom connected to CH_3 and the second one is on the σ orbital of the hydrogen-less carbon in the ring. The energies of **B3** and **B3o** are close. At the B3LYP and RCCSD(T) levels, **B3o** is slightly more stable, but at the G2M level **B3** lies 1.4 kcal/mol lower than **B3o**. It is worth mentioning that we used for geometry optimization of **B3o** the unrestricted B3LYP (UB3LYP) method. This approach has been shown recently[21] to give geometry of such biradical as prefulvene in good agreement with the results of multireference CASSCF calculations.

Another path from **B2** to **B3** would involve two successive 1,2-H shifts via isomer **B4**, instead of one 1,3-H shift. **B4** is also a biradical structure with one unpaired electron on the hydrogen-less carbon of the ring and the second electron on the carbon of the CH_2 group. The energy of **B4** is high, 122.9 kcal/mol relative to benzene at the G2M level. The search of the transition state for the 1,2-hydrogen shift between **B2** and **B4** gives TS **2**. TS **2** exhibits a bicyclic geometry and connects **B4** not with fulvene but with isofulvene or bicyclo[3.1.0]hexa-1,3-diene. The energy of TS **2**, 141.4 kcal/mol at the G2M level relative to benzene, is significantly higher than that of TS **1**. Isomer **B4** can be formed from the bicyclo[3.1.0]hexa-1,3-diene without the hydrogen shift, by the cleavage of one of the CC bonds in the three-member ring cycle. At the B3LYP level with ZPE corrections, the energy of the corresponding TS **3** is slightly lower than the energy of TS **1**. According to our earlier results,[21] isofulvene lies 41.3 kcal/mol higher than fulvene and isomerizes to **B2** with a very low barrier. On the other hand, a TS search for the 1,2-hydrogen shift between **B4** and **B3**

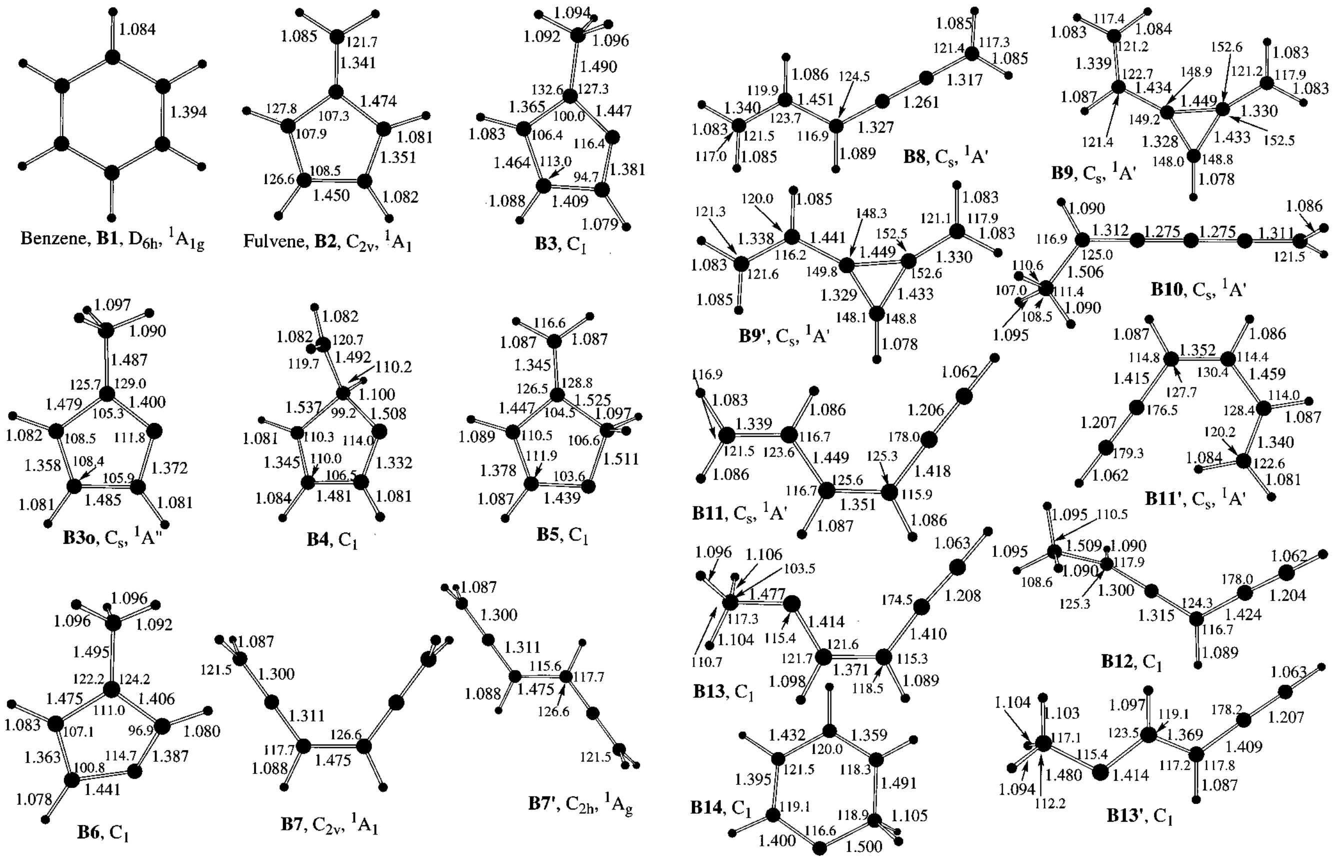

Figure 2. Geometries of various isomers of C_6H_6 optimized at the B3LYP/6-311G(d,p) level. (Bond lengths are in angstroms, bonds angles are in degrees.)

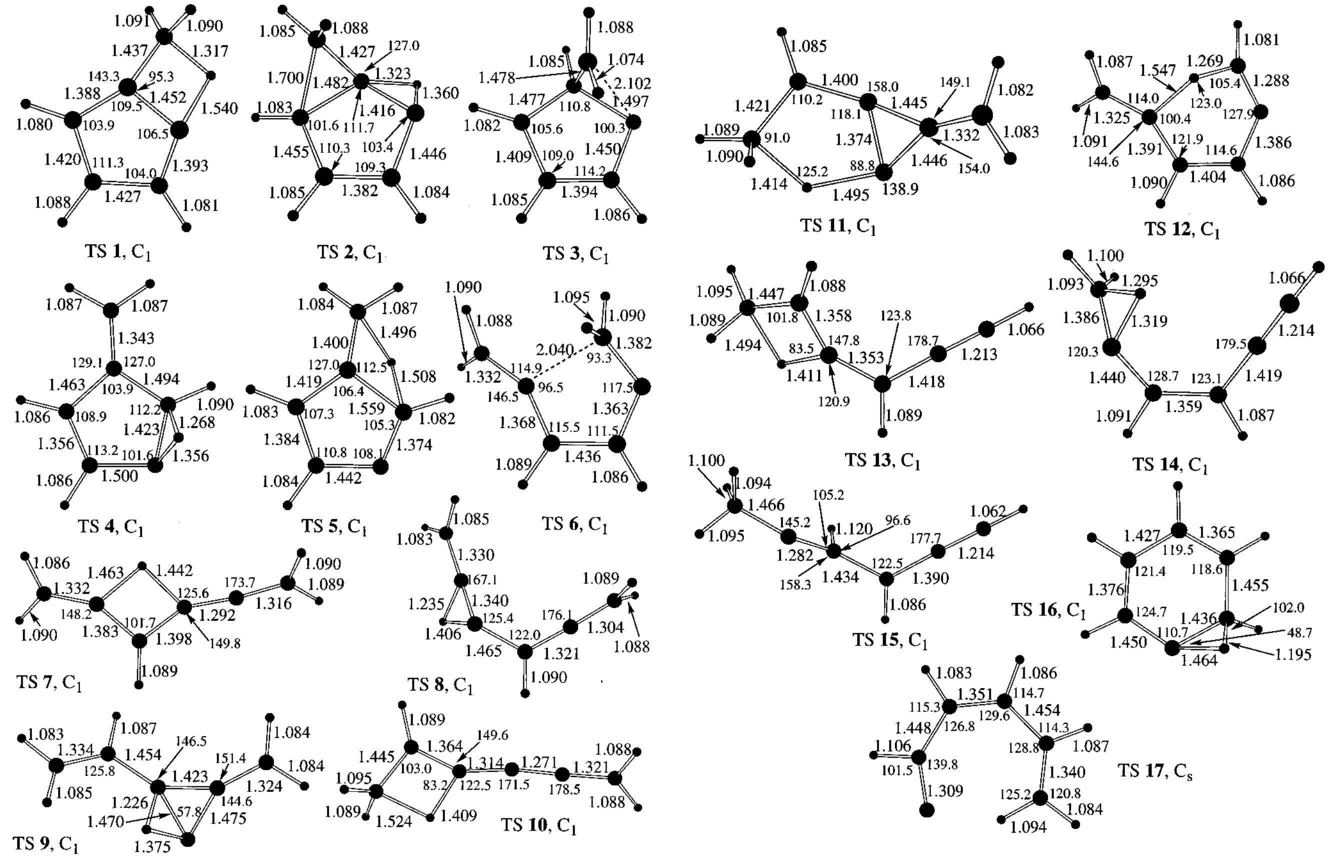

Figure 3. Geometries of various transition states along the $C_6H_6 \rightarrow C_5H_3 + CH_3$ reaction optimized at the B3LYP/6-311G(d,p) level. (Bond lengths are in angstroms, bonds angles are in degrees).

converges to TS **1**, which actually connects **B2** and **B3**. Therefore, isomer **B4** is not relevant to the $C_6H_6 \rightarrow C_5H_3 + CH_3$ reaction. **B4** can be formed from isofulvene but cannot directly isomerize to **B3**. The **B4** → **B3** rearrangement can

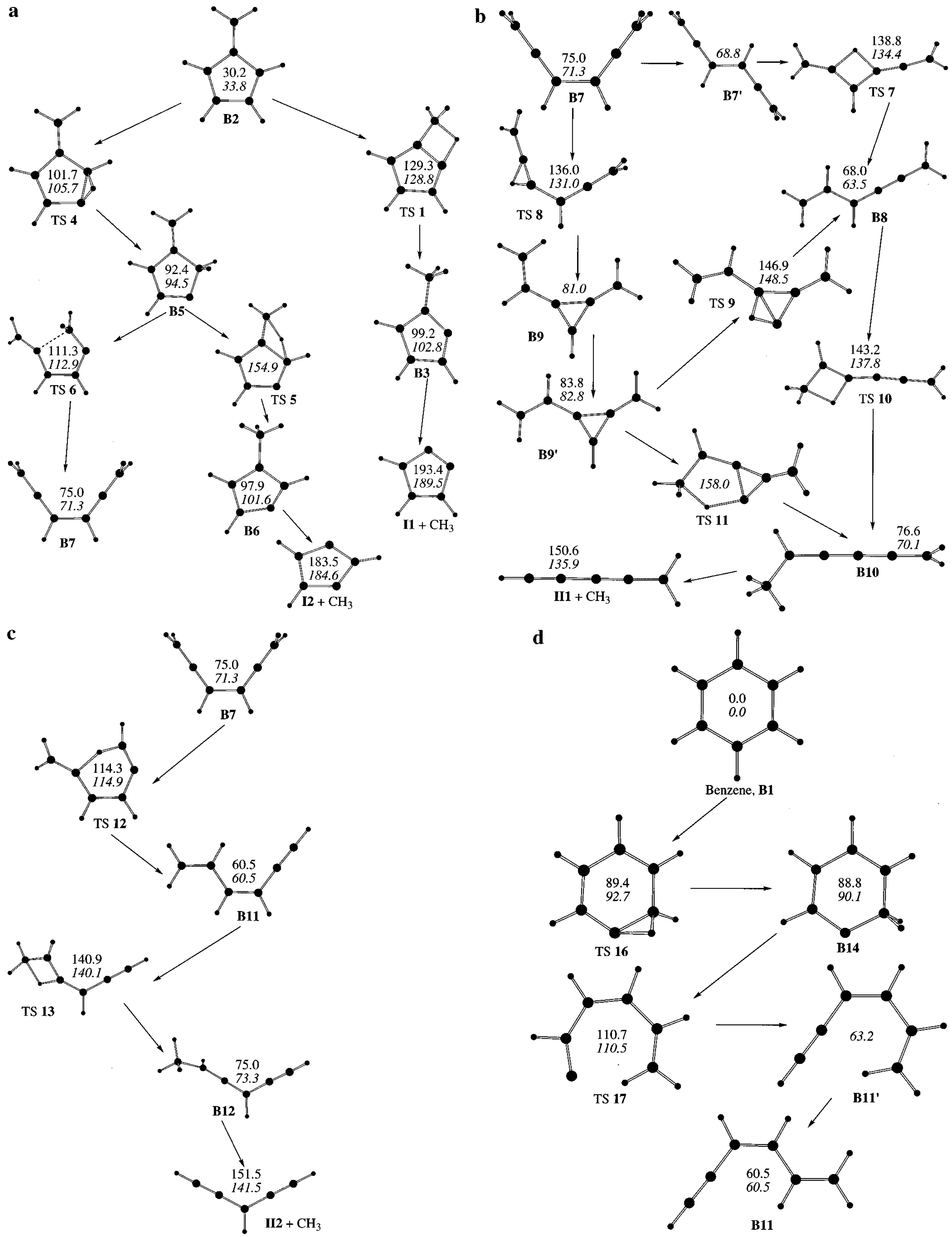

Figure 4. (a) Mechanisms of the formation of C_5H_3 **I1** and **I2** and ring opening in fulvene; (b) mechanisms of the formation of $H_2CCCCCH$ **II1** from the open-chain isomer **B7**; (c) mechanism of the formation of HCCC(H)CCH **II2** from the open-chain isomer **B7**; (d) mechanism of the formation of the open-chain isomer $CH_2{=}CHCH{=}CHC{\equiv}CH$ **B11** directly from benzene. Plain and italic numbers show the energies relative to benzene, calculated at the G2M and B3LYP+ZPE levels of theory, respectively.

proceed only by the following pathway: **B4** → TS **2** or **3** → bicyclo[3.1.0]hexa-1,3-diene → fulvene → TS **1** → **B3**.

As seen in Figure 4a, formation of C_5H_3 **I2** takes place as follows: **B2** → TS **4** → **B5** → TS **5** → **B6** → **I2** + CH_3. The reaction begins with a 1,2-H shift in the ring which is followed by the 1,3-hydrogen shift and the cleavage of the single CC bond. The barrier for the 1,2-H shift at TS **4** is 71.6 kcal/mol at the G2M level, about 25 kcal/mol lower than the barrier for the 1,3-H shift at TS **1**. Isomer **B5** formed after TS **4** is cleared has a carbene-like electronic structure. The second step of the mechanism requires a much higher energy; TS **5** is by 154.9 kcal/mol higher than benzene in the B3LYP + ZPE approximation. The electronic structure of isomer **B6** is similar to one of the resonance structures of C_5H_3 **I2** discussed in the previous section, but with an additional out-of-ring CC bond. The strength of this bond is calculated to be 85.5 kcal/mol at the G2M level, and the total energy loss in the **B1** → **I2** + CH_3 reaction is 183.5 kcal/mol. The last step of this mechanism, the rupture of the out-of-ring CC bond in **B6**, occurs endothermically without reverse barrier.

C_5H_3 **I2** is not likely to be formed from fulvene because of the very high barrier at TS **5**. From intermediate **B5**, the reaction is expected to proceed by another mechanism, ring opening and formation of an open-chain structure. TS **6** is the transition state for the rupture of one of the CC bonds in the ring of **B5** to produce the open-chain isomer **B7**. The barrier is relatively low, 18.9 kcal/mol with respect to **B5**; TS **6** lies 111.3 kcal/mol higher than benzene at the G2M level and 42 kcal/mol lower than TS **5** at the B3LYP + ZPE level. Interestingly, TS **6** was found while we searched for a TS for the 1,2-hydrogen shift in **B5**. The **B5** → **B6** isomerization cannot occur by two sequential 1,2-H shifts. Instead, the system prefers ring opening and formation of **B7**.

The open-chain isomer **B7**, 1,2,4,5-hexatetraene, is 75.0 kcal/mol less stable than benzene. **B7** can serve as a precursor for the formation of the most stable open-chain structures of the C_5H_3 radical, **II1** and **II2**, and, on the other hand, can produce C_3H_3 + C_3H_3 by the cleavage of the single CC bond. Various reaction pathways leading from **B7** to **II1** are illustrated in Figure 4b. Rotation around the single CC bond in **B7** gives another conformation of the 1,2,4,5-hexatetraene, **B7′**. **B7** and **B7′** have C_{2v} and C_{2h} symmetry, respectively. **B7′** is 2.5 kcal/mol more stable than **B7** at the B3LYP + ZPE level. We do not consider here the barrier for rotation about the single CC bond because it is expected to be much lower than the barriers for the hydrogen shifts. 1,3-H shift in **B7′** via TS **7** leads to isomer **B8**, 1,3,4,5-hexatetraene. **B8** is 7.0 kcal/mol more stable than **B7** and lies 68.0 kcal/mol higher than benzene at the G2M level of theory. The sigmatropic 1,3-H shift in **B7′** is a symmetry-forbidden process for suprafacial geometry in the π systems.[36] The barrier at TS **7** is 65.5 kcal/mol at the B3LYP + ZPE level with respect to **B7′**, and the transition state lies by 138.8 kcal/mol higher than benzene at the G2M level. Intermediate **B8** can further undergo another 1,3-hydrogen shift which leads to **B10**, 2,3,4,5-hexatetraene. The barrier at TS **10** is high again, 75.2 kcal/mol relative to **B8** at the G2M level. **B10** is 1.6 and 76.6 kcal/mol less stable than **B7** and benzene **B1**, respectively. Elimination of the CH_3 group in **B10** without a barrier leads to C_5H_3 **II1**. The CC single bond strength in **B10** is found to be only 74.0 kcal/mol. The bond is quite weak, which can be attributed to the fact that **II1** is additionally stabilized by the presence of several resonance structures, as discussed in the previous section. The overall mechanism of formation of **II1** from fulvene can be written as follows: **B2** → TS **4** → **B5** → TS **6** → **B7** → **B7′** → TS **7** → **B8** → TS **10** → **B10** → **II1** + CH_3. The highest transition state on this pathway is TS **10**, lying 143.2 kcal/mol higher than benzene in the G2M approximation.

Intermediate **B8** can also be formed by another mechanism. 1,2-H shift in **B7** via TS **8** leads to isomer **B9**. Although the 1,2-hydrogen shift is symmetry-allowed, the barrier at TS **8** is still high, 61.1 kcal/mol. At the G2M level, TS **8** is only 2.7 kcal/mol lower than TS **7**. Isomer **B9** has a geometry with a three-member carbon ring. Thus, the 1,2-H shift from **B7** to **B9** is accompanied by the cyclization. **B9** has a stability comparable to those of **B7** and **B10**. Rotation about the single CC bond in **B9** gives **B9′**. At the B3LYP + ZPE level, **B9′** is 1.8 kcal/mol higher in energy than **B9**. In the next step, **B8** is formed by the second 1,2-hydrogen shift via TS **9**. The barrier for the hydrogen shift is 63.1 kcal/mol with respect to **B9′** at the G2M level. TS **9** lies 8.1 kcal/mol higher than TS **7**. Hence, the multistep mechanism for the formation of **B8**, **B7** → TS **8** → **B9** → **B9′** → TS **9** → **B8** is less favorable than the **B7** → **B7′** → TS **7** → **B8** mechanism. From **B9′**, the reaction may proceed directly to **B10**, by the 1,4-hydrogen shift at TS **11**. However, the barrier is too high; at the B3LYP + ZPE level TS **11** lies 158.0 kcal/mol higher than benzene. Thus, the shortest and lowest in energy pathway from **B7** to **B10** involves two successive 1,3-hydrogen shifts.

Mechanism of the formation of C_5H_3 **II2** starting from **B7** is shown in Figure 4c. In the first step, the 1,5-hydrogen shift takes place. The barrier at TS **12** is relatively low, 39.3 kcal/mol with respect to **B7**, i.e., 21.8 and 24.5 kcal/mol lower than the barriers for the 1,2-H shift at TS **8** and the 1,3-H shift at TS **7**. After the 1,5-hydrogen shift, intermediate **B11** is formed, 1,3-hexadien-5-yne. **B11** is 60.5 kcal/mol less stable than benzene at the G2M level. 1,3-H shift in **B11** via TS **13** leads to isomer **B12**, 2,3-hexadien-5-yne. The barrier is 70.4 kcal/mol relative to **B11**, and TS **13** lies 140.9 kcal/mol higher than benzene. The stability of **B12** is similar to that of **B7**. Finally, splitting the single CC bond in **B12** results in C_5H_3 **II2** + CH_3. This step has no barrier because the reverse reaction is a radical−radical association. The CC bond strength in **B12** is 76.6 kcal/mol in the G2M approximation, and the product, **II2** + CH_3, lies 151.5 kcal/mol higher than fulvene. Because the barrier for the 1,3-H shift at TS **13** is high, we investigated additionally the possibility of the **B11** → **B12** rearrangement by two successive 1,2-hydrogen shifts. The first 1,2-H shift in **B11** occurs via TS **14**. The energy of this transition state is 133.5 kcal/mol relative to benzene, i.e., 7.3 kcal/mol lower than the energy of TS **13**. After TS **14** is cleared, isomer **B13** is formed, which has a carbene-like structure. **B13** lies 127.9 kcal/mol higher than benzene at the G2M level. Despite the careful search, we could not find a transition state for the 1,2-H shift in **B13** leading to **B12**. The optimization always converged to TS **15**, which is a transition state for the rotation around the double CC bond and connects **B13** and **B13′**. The energy of TS **15** is 144.0 kcal/mol relative to benzene at the B3LYP + ZPE level. Therefore , we concluded that the system cannot get directly from **B13** to **B12**, instead, the isomerization has to proceed by the **B13** → TS **14** → **B11** → TS **13** → **B12** pathway. Thus, the lowest in energy mechanism of formation of C_5H_3 **II2** from fulvene is the following: **B2** → TS **4** → **B5** → TS **6** → **B7** → TS **12** → **B11** → TS **13** → **B12** → **II2** + CH_3, and the highest point on the path before the products is TS **13**, 140.9 kcal/mol with respect to benzene.

Next we consider a reaction mechanism which leads to C_5H_3 directly from benzene bypassing fulvene. Melius et al.[37] first suggested that the ring opening in benzene can lead directly to $CH_2{=}CHCH{=}CHC{\equiv}CH$ (**B11′**) via a $CH_2{=}CHCH{=}CH{-}CH{=}C{:}$ transition state. Figure 4d illustrates the details of this mechanism. At the first step, a 1,2-H shift in benzene gives a cyclohexadiene carbene intermediate **B14** via TS **16**. **B14** is 88.8 kcal/mol less stable than **B1** at the G2M level and is separated from benzene by a low barrier of only 0.6 kcal/mol. In the next step, the ring opening accompanied by another 1,2-H shift takes place at TS **17**. At the G2M level TS **17** is 110.7 kcal/mol higher relative to benzene, i.e., slightly lower in energy than TS **6**, another transition state for the ring opening. After this transformation **B11′** is formed, which is 4.2 kcal/mol less stable than **B11** at the B3LYP + ZPE level. Rotation around a single CC bond in **B11′** produces **B11**. Consequently, **B11** can isomerize and dissociate to $C_5H_3 + CH_3$ by the following mechanisms, **B11** → TS **13** → **B12** → C_5H_3 **II2** + CH_3 and **B11** → TS **12** → **B7** → **B7′** → TS **7** → **B8** → TS **10** → **B10** → C_5H_3 **II1** + CH_3, which have been discussed in detail above.

Concluding Remarks

Various isomers of the C_5H_3 radical are investigated. The most stable structures are found to be **II1**, $H_2CCCCCH$, and **II2**, HCCC(H)CCH, where **II1** is 1.0 kcal/mol lower in energy than **II2** at our best G2M level of theory. The isomer **III1**, ethynyl cyclopropenyl radical, the most stable structure for the cationic species, lies 30.3 kcal/mol higher than **II1**. Of the five-member ring isomers, the most favorable structure is **I2** having an across-ring CC bond, which is 32.9 kcal/mol less stable than **II1**. The calculated endothermicity of the benzene → $H_2CCCCCH + CH_3$ reaction is 150.6 kcal/mol.

The mechanisms of the dissociation of C_6H_6 leading to different isomers of C_5H_3 are also studied. After isomerization of benzene to fulvene, **II1** can be formed by the following pathway: fulvene **B2** → TS **4** → **B5** → TS **6** → **B7** → **B7′** → TS **7** → **B8** → TS **10** → **B10** → $H_2CCCCCH$ **II1** + CH_3. The highest barrier is found for the 1,3-hydrogen shift at TS **10** which lies 143.2 kcal/mol higher in energy than benzene. The mechanism of the formation of **II2** shares the first few steps with the pathway leading to **II1**, until the ring opens up and the 1,2,4,5-hexatetraene isomer **B7** is formed. Starting from **B7**, the following path leads to **II2**: **B7** → TS **12** → **B11** → TS **13** → **B12** → HCCC(H)CCH **II2** + CH_3. The highest in energy transition state is TS **13**, 140.9 kcal/mol above benzene. The last step in both mechanisms, splitting the single C−C bond, takes place endothermically without a reverse barrier. **B11** can also be produced directly from benzene by the **B1** → TS **16** → **B14** → TS **17** → **B11′** → **B11** mechanism. The reaction mechanisms for the dissociation of benzene producing **II1** and **II2** are expected to compete. The highest barriers of these mechanisms involve hydrogen shifts; therefore, tunneling would enhance the reaction rates for isomerization or make the reaction happen. Of the open-chain isomers of C_6H_6, calculated in the present study, the most stable structure is **B11**, 1,3-hexadien-5-yne, which lies 60.5 kcal/mol higher than benzene.

According to our calculations, the $C_5H_3 + CH_3$ channel of the dissociation of benzene requires at least about 150 kcal/mol of available energy, which is much higher than the energy of a 248 nm photon. The energy of two photons is sufficient for the formation of $C_5H_3 + CH_3$. This result implies that this channel of benzene photodissociation is most likely a two-photon process.

Acknowledgment. A.M.M. is grateful to Academia Sinica for the fellowship at IAMS. This work supported in part by the National Science Council of ROC. We thank Mr. D. Blank for providing us new experimental data concerning the $C_5H_3 + CH_3$ of benzene photodissociation.

References and Notes

(1) Yokoyama, A.; Zhao, X.; Hintsa, E. J.; Continetty, R. E.; Lee, Y. T. *J. Chem. Phys.* **1990**, *92*, 4222.

(2) (a) Reeher, J. R.; Flesch, G. D.; Svec, H. J. *Org. Mass Spectrom.* **1976**, *11*, 154. (b) Reeher, J. R.; Flesch, G. D.; Svec, H. J. *Int. J. Mass Spectrom. Ion Phys.* **1976**, *19*, 351.

(3) Momigny, J.; Brakier, L.; D'Or, L. *Bull. Cl. Sci., Acad. R. Belg.* **1962**, *48*, 1002.

(4) Franklin, J. L.; Carroll, S. R. *J. Am. Chem. Soc.* **1969**, *91*, 5940; *Ibid.* **1969**, *91*, 6564.

(5) Dannacher, J.; Heilbronner, E.; Stadelmann, J. P.; Vogt, J. *Helv. Chim. Acta* **1979**, *62*, 2186.

(6) El-Sayed, M. A.; Tai, T. L. *J. Phys. Chem.* **1988**, *92*, 5333.

(7) Östürk, F.; Moini, M.; Brill, F. W.; Eyler, J. R.; Buckley, T. J.; Lias, S. G.; Ausloos, P. J. *J. Phys. Chem.* **1989**, *93*, 4038.

(8) Selim, E. T. M.; Rabbih, M. A.; Fahmey Ahmad, M. A.; Shalibi, A. S. *Arab Gulf. J. Sci. Res.* **1989**, *7*, 53.

(9) Jochims, H. W.; Rasekh, H.; Ruehl, E.; Baumgaertel, H.; Leach, S. *Chem. Phys.* **1992**, *168*, 159.

(10) Kompe, B. M.; Peel, J. B.; Traeger, J. C. *Org. Mass Spectrom.* **1993**, *28*, 1253.

(11) Abouelaziz, H.; Gomet, G. C.; Pasquerault, D.; Rowe, B. R.; Mitchell, J. B. A. *J. Chem. Phys.* **1993**, *99*, 237.

(12) Fucaloro, A. F.; Srivastava, S. K. *J. Braz. Chem. Soc.* **1994**, *4*, 7.

(13) Rowe, B. R.; Canosa, A.; Sims, A. R. *J. Chem. Soc., Faraday Trans.* **1993**, *89*, 2193.

(14) Calcote, H. F. Mechanisms of Soot Nucleation in Flames—A Critical Review. *Combust. Flame* **1981**, *42*, 215.

(15) Lammertsma, K.; Schleyer, P. v. R. *J. Am. Chem. Soc.* **1983**, *105*, 1049.

(16) Weiner, B.; Williams, C. J.; Heaney, D.; Zerner, M. C. *J. Phys. Chem.* **1990**, *94*, 7001.

(17) Kuehnel, W.; Gey, E.; Ondruschka, B. *Z. Phys. Chem. (Leipzig)* **1987**, *268*, 805.

(18) Pasto, D. J. *J. Am. Chem. Soc.* **1988**, *110*, 8164.

(19) (a) Melius, C. F. In *Chemistry and Physics of Energetic Materials*; Bulusu, S. N., Ed.; Kluwer Academic Publishers: Dordrecht, 1990; p. 21. (b) Ho, P.; Melius, C. F. *J. Phys. Chem.* **1990**, *94*, 5120. (c) Allendorf, M. D.; Melius, C. F. *J. Phys. Chem.* **1993**, *97*, 720.

(20) Mebel, A. M.; Morokuma, K.; Lin, M. C. *J. Chem. Phys.* **1995**, *103*, 7414.

(21) Madden, L. K.; Mebel, A. M.; Lin, M. C.; Melius, C. F. *J. Phys. Org. Chem.* **1996**, *9*, 801.

(22) (a) Becke, A. D. *J. Chem. Phys.* **1993**, *98*, 5648. (b) *Ibid.* **1992**, *96*, 2155. (c) *Ibid.* **1992**, *97*, 9173.

(23) Lee, C.; Yang, W.; Parr, R. G. *Phys. Rev.* **1988**, *B37*, 785.

(24) Krishnan, R.; Frisch, M.; Pople, J. A. *J. Chem. Phys.* **1980**, *72*, 4244.

(25) (a) Curtiss, L. A.; Raghavachari, K.; Trucks, G. W.; Pople, J. A. *J. Chem. Phys.* **1991**, *94*, 7221. (b) Pople, J. A.; Head-Gordon, M.; Fox, D. J.; Raghavachari, K.; Curtiss, L. A. *J. Chem. Phys.* **1989**, *90*, 5622. (c) Curtiss, L. A.; Jones, C.; Trucks, G. W.; Raghavachari, K.; Pople, J. A. *J. Chem. Phys.* **1990**, *93*, 2537.

(26) (a) Purvis, G. D.; Bartlett, R. J. *J. Chem. Phys.* **1982**, *76*, 1910. (b) Hampel, C.; Peterson, K. A.; Werner, H.-J. *Chem. Phys. Lett.* **1992**, *190*, 1. (c) Knowles, P. J.; Hampel, C.; Werner, H.-J. *J. Chem. Phys.* **1994**, *99*, 5219. (d) Deegan, M. J. O.; Knowles, P. J. *Chem. Phys. Lett.* **1994**, *227*, 321.

(27) Frisch, M. J.; Trucks, G. W.; Schlegel, H. B.; Gill, P. M. W.; Johnson, B. G.; Robb, M. A.; Cheeseman, J. R.; Keith, T.; Petersson, G. A.; Montgomery, J. A.; Raghavachari, K.; Al-Laham, M. A.; Zakrzewski, V. G.; Ortiz, J. V.; Foresman, J. B.; Cioslowski, J.; Stefanov, B. B.; Nanayakkara, A.; Challacombe, M.; Peng, C. Y.; Ayala, P. Y.; Chen, W.; Wong, M. W.; Andres, J. L.; Replogle, E. S.; Gomperts, R.; Martin, R. L.; Fox, D. J.; Binkley, J. S.; Defrees, D. J.; Baker, J.; Stewart, J. P.; Head-Gordon, M.; Gonzalez, C.; Pople, J. A. *GAUSSIAN 94*, Revision B.2; Gaussian, Inc.: Pittsburgh: PA, 1995.

(28) MOLPRO is a package of *ab initio* programs written by H.-J. Werner and P. J. Knowles, with contributions from J. Almlöf, R. D. Amos, M. J. O. Deegan, S. T. Elbert, C. Hampel, W. Meyer, K. Peterson, R. Pitzer, A. J. Stone, P. R. Taylor, and R. Lindh.

(29) Lias, S. G.; Bartmess, J. E.; Liebman, J. F.; Holmes, J. L.; Levin, R. D.; Mallard, W. G. *J. Phys. Chem. Ref. Data* **1988**, *17*, Suppl. 1.

(30) Hehre, W. J.; Radom, L.; Schleyer, P. v. R.; Pople, J. *Ab Initio Molecular Orbital Theory*; Wiley: New York, 1986.

(31) Baird, N. C. *Mol. Phys.* **1970**, *18*, 39.

(32) Chase, M. W., Jr.; Davles, C. A.; Downey, J. R., Jr.; Frurip, D. J.; McDonald, R. A.; Syverud, A. N. JANAF Thermochemical Tables. *J. Phys. Chem. Ref. Data* **1985, *14*,** Suppl. 1.

(33) Klessinger, M.; Michl, J. *Excited States and Photochemistry of Organic Molecules*; VCH: New York, 1995 and references therein.

(34) Palmer, I. J.; Ragazos, I. N.; Bernardi, F.; Olivucci, M.; Robb, M. A. *J. Am. Chem. Soc.* **1993**, *115*, 673.

(35) (a) Dreyer, J.; Klessinger, M. *J. Chem. Phys.* **1994**, *101*, 10655. (b) Dreyer, J.; Klessinger, M. *Chem. Eur. J.* **1996**, *2*, 335.

(36) Isaacs, N. S. *Physical Organic Chemistry*; Wiley: New York, 1987.

(37) Melius, C. F.; Miller, J. A.; Evleth, E. M. *Twenty-Fourth Symposium (International) on Combustion*; The Combustion Institute: Pittsburgh, PA, 1992; p 621.